# Interfacial Ordering of Tristearin Induced by Glycerol Monooleate and PGPR: A Coarse-Grained Molecular Dynamics Study

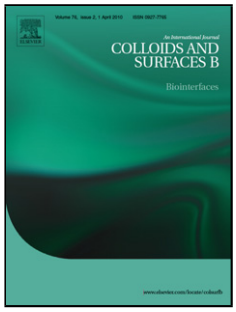


Title: Interfacial Ordering of Tristearin Induced by Glycerol Monooleate and PGPR: A Coarse-Grained Molecular Dynamics Study

Author: Nicole L. Green Stephen R. Euston Dérick Rousseau

PII: S0927-7765(19)30182-1
DOI: https://doi.org/doi:10.1016/j.colsurfb.2019.03.033
Reference: COLSUB 10083

To appear in: *Colloids and Surfaces B: Biointerfaces*

Received date: 1 October 2018
Revised date: 13 March 2019
Accepted date: 14 March 2019

Please cite this article as: Nicole L. Green, Stephen R. Euston, Dérick Rousseau, Interfacial Ordering of Tristearin Induced by Glycerol Monooleate and PGPR: A Coarse-Grained Molecular Dynamics Study, *<![CDATA[Colloids and Surfaces B: Biointerfaces]]>* (2019), https://doi.org/10.1016/j.colsurfb.2019.03.033

- Both GMO and PGPR displace tristearin from the water interface
- Adsorbed GMO acyl chains act as a template for nucleation of tristearin crystals at the interface
- PGPR disorders tristearin acyl chains at the interface

**Manuscript Title**: Interfacial Ordering of Tristearin Induced by Glycerol Monooleate and PGPR: A Coarse-Grained Molecular Dynamics Study

Authors: Nicole L. Green, Stephen R. Euston, Dérick Rousseau

Words: 5354

Figures: 8

# Interfacial Ordering of Tristearin Induced by Glycerol Monooleate and PGPR: A Coarse-Grained Molecular Dynamics Study

Nicole L. Green[a], Stephen R. Euston[b,*], Dérick Rousseau[a,**]

[a] *Department of Chemistry & Biology, Ryerson University, Toronto, Canada*
[b] *Institute of Mechanical, Process & Energy Engineering, School of Engineering & Physical Sciences. Heriot-Watt University, Edinburgh, Scotland*

**Abstract**

We use coarse-grained molecular dynamics simulations to study the effect of surfactant structure on the ordering of bulk tristearin at an oil-water interface. In the absence of surfactant, tristearin acyl chains are marginally aligned normal to the interface. The surfactant glycerol monooleate (GMO), a common small-molecule monoacylglycerol (MW: 357 g/mol), preferentially adsorbs to the oil-water interface, displacing more of the tristearin as its concentration increases. The tristearin that remains at the interface is closely aligned normal to the interface. Adjacent to the interface, bulk tristearin increasingly aligns with its acyl chains entwined with the GMO acyl chain, which also preferentially aligns normal to the interface. In contrast, polyglycerol polyricinoleate (PGPR), a bulkier, polymeric surfactant (MW: 1398 g/mol for a molecule with five monomers), both displaces tristearin from the interface and reduces the alignment of the molecules that remain. We suggest that the similar fatty acid moieties of GMO (oleic acid) and tristearin (stearic acid) lead to liquid-state association and alignment, the latter of which can then serve as a template onto which tristearin crystals can nucleate. Conversely, by both displacing tristearin from the interface and reducing alignment below that of the surfactant-free sys-

*Corresponding author
**Corresponding author
*Email addresses:* S.R.Euston@hw.ac.uk (Stephen R. Euston), rousseau@ryerson.ca (Dérick Rousseau)

tem, PGPR eliminates the possibility of tristearin interfacial crystallisation.

*Keywords:* molecular dynamics, simulation, surfactant, triacylglycerol, interface, adsorption

## 1. Introduction

Water-in-oil (W/O) emulsions are prevalent in industries including pharmaceuticals (drug delivery systems), cosmetics, and foods [1, 2, 3]. Fats in foods have shown two distinct modes of W/O stabilisation - network and interfacial (Pickering-type) [4]. In butter, for example, solid triacylglycerol (TAG) crystals create a network in the continuous phase that effectively locks water droplets in place.

TAG crystals are not inherently driven to the oil-water interface but can be made surface-active by the adsorption of surfactants [5]. Surfactants such as saturated monoacylglycerols (MAGs) can also crystallise at the oil-water interface, creating a solid Pickering shell around a water droplet [6]. At a fixed solid fat content (SFC), it has been shown that Pickering stabilisation from saturated MAGs is more effective against sedimentation than TAG networks [7]. Both saturated MAGs and TAGs can be used together to achieve combined network and Pickering stabilisation.

What remains unclear is the role that unsaturated MAGs and other liquid-state surfactants have on fat crystallisation in W/O emulsions. As they remain liquid at room temperature, they cannot form a solid shell around water droplets. Still, due to their molecular similarity with TAG molecules, unsaturated MAG fatty acid chains are capable of accelerating TAG nucleation and growth in bulk fat, albeit to a lesser extent than saturated MAGs [8]. Another commonly-used liquid-state food surfactant, polyglycerol polyricinoleate (PGPR), occupies a greater surface area per molecule due to its branched structure [9] and lacks any obvious acyl chain complementarity with TAG molecules. Results remain inconclusive, with some reporting that PGPR orders TAG crystals at the interface [10] while others have seen no interfacial crystallisation of

TAG molecules in PGPR-stabilised droplets [11].

Evidence of a templating effect has been shown in liquid crystal systems: surfactants at the water-liquid crystal interface can induce ordering in the bulk liquid crystal at both curved [12] and planar [13] interfaces. Surfactant structure has been shown to affect the resulting liquid crystal director, with tail branching [14] or looped conformations [15] unable to affect the natural planar ordering of liquid crystals at the interface. Surfactants with long linear alkyl chains at concentrations near monolayer coverage are better suited to induce homeotropic liquid crystal ordering due to penetration of liquid crystal molecules into the surfactant layer [15]. A similar effect has been reported at the alkane-water interface: incorporation of short chains into the surfactant layer leads to surfactant tails orienting more perpendicularly to the interface compared to the air/water interface [16]. The interpenetration of bulk oil molecules into a surfactant layer reduces Van der Waals attraction between the latters alkyl chains, leading to greater disorder in the form of gauche defects along the surfactant tail [17].

Molecular dynamics simulations have been used extensively to study the adsorption of surfactants at fluid interfaces. However, there have been very few studies on the TAG-water interface. Hughes & Walsh (2015) claim the first all-atom simulation of the TAG-water [tristearin(TS)-water] interface modelled as a TS bilayer in contact with water, and the adsorption of sodium dodecylbenzene sulphate (SDBS) to it [18]. SDBS molecules were found to spontaneously insert into the TS layer, but only had a moderate effect on the structure of the layer. More recently, coarse-grained (CG) molecular dynamics (MD) has been applied to TAG-water interface and surfactant adsorption at oil-water interfaces. This allows larger system sizes and longer simulations times at the expense of atomic detail. Simulations using the Martini CG force field to explore the adsorption of sodium dodecyl sulphate (SDS) at a hydrocarbon-implicit water interface have indicated two adsorption mechanisms  SDS either adsorbs as whole micelles or as individual molecules that have separated from the micelles [19, 20]. CG MD simulations of mixed TAG and partial acylglycerol systems in the presence of

water have shown that as water content increased, a phase transition to separate lipid and water phases was observed, accompanied by an increase in the second rank order parameter of the lipid acyl chains as the acyl chains aligned at the lipid-water interface [21].

In this study, we used CG MD simulations to explore the oil-water and air-water interfaces in the presence of either glycerol monooleate (GMO) or PGPR. We expected their different molecular structures to affect their ability to promote ordering of neighbouring TAG in the bulk oil phase. We also varied the surfactant concentration to study how surface coverage affects molecular ordering and further, if that ordering will extend into the bulk phase.

## 2. Materials and Methods

CG MD simulations were carried out using the Gromacs MD package version 4.0.5 [22] and the Martini coarse-grained lipid force field [23].

CG topologies for GMO and TS were defined by modifying the topology for triolein originally proposed by Vuorela et al. [24], which uses a 3:1 or 4:1 atom:CG bead mapping of the Martini force field, by replacing *cis* C=C with a single bond. A TS CG molecule consisted of a single glycerol bead (GOH), three beads representing each ester link to the GOH, and three acyl chains (one acyl chain per ester link see Figure 1) of five $CH/CH_2/CH_3$ beads. Similarly, the GMO molecule was defined by taking the triolein and removing two of the ester beads and the two attached acyl chains. Thus, the GMO consisted of one GOH bead, one ester link bead, and five $CH_2/CH_3$ beads (Figure 1). The bond angle between the $2^{nd}$, $3^{rd}$, and $4^{th}$ acyl chain beads was defined as 120° (compared to 180° in the stearate chain from which the topology was modified) to account for the *cis* C=C found in oleate chains. The GOH bead for GMO was defined as having a higher polarity than the GOH bead for TS, reflecting the presence of the two hydroxyl groups that are esterified in TS. The PGPR CG structure was constructed using the a 3:1 or 4:1 mapping of the Martini force field and comprised of five repeat units of the molecule. Assignment of CG beads was

made based on a comparison with already parametrised molecules of a known structure.

To construct GMO or PGPR monolayers at the TS-water interface, the following procedure was used. Two monolayers of GMO or PGPR [with GMO numbers varied in the range 100-800 (50-400 per interface) or PGPR 40-200 (20-100 per interface)] were constructed by arranging the GMO molecules into two ordered layers within a periodic rectangular box. The maximum number of GMO per interface (400) was sufficient to give a GMO surface coverage of 1.67 mg/m$^2$ which is below the saturation surface coverage for GMO [25]. A total of 900 TS molecules were inserted in the space between the monolayers, and water was added on the other side of the monolayer to a density of 1000 g/L. The numbers of TS and water molecules were determined by trial and error to give a density close to that of each molecule at 300K. The conformation was energy-minimised using a conjugate gradients algorithm. The system was equilibrated for a short 20 ps simulation using an NPT ensemble (P = 1 bar, T = 300K, Parrinello-Rhaman barostat [26, 27]) and V-rescale thermostat [28]. The average box size after the system pressure had equilibrated to 1 bar was noted. Production runs of 600 ns were carried out with the box size fixed to the average box size at 1 bar pressure, using an NVT ensemble (T = 300K, V-rescale thermostat). Several were run for 1200 ns to verify that, by 600 ns, systems had successfully equilibrated. In this short time, we saw no evidence of TS crystallisation even though the temperature (300K) was below the melting point of TS, suggesting that the simulation was carried out under supercooled conditions. This is not unusual in MD simulations as the short timescales and small system sizes that are used preclude the formation of nucleation points for crystallisation unless controlled quenching from high to low temperature (a technique unsuitable for our interfacial system) is used [29, 30]. The non-bonded interactions were defined using the Martini CG lipid force field [23]. To verify that this method of forming the GMO monolayer did not affect the monolayer structure, we also carried out a simulation where 200 GMO molecules were allowed to freely adsorb onto the TS-water interface from the TS phase then

equilibrate using the method above. After simulating for 600 ns, the density profiles obtained from this simulation were virtually superimposable with those resulting from the simulations of pre-formed GMO monolayers (see Figure S?? supplementary information). The lone difference between the two simulations was that, in the freely adsorbing system, not all GMO molecules adsorbed even if the simulation was extended to 1500 ns. This led to the two interfaces having unequal numbers of GMO. Since the structure of the interface appeared to be unaffected by the method used to form it, and to avoid unequal GMO numbers at the two interfaces, we chose to use constructed monolayers for all GMO and PGPR concentrations.

The average order parameters normal to the interface were determined for the acyl chains of the TS molecule and of the GMO acyl chain using Equation 1 [31].

$$S_{CD} = \frac{1}{2}\langle 3cos^2\theta - 1\rangle \quad (1)$$

Here, $\theta$ is the angle between a vector representing the bond between two adjacent carbon atoms and a vector in the direction of the z-axis perpendicular to the interface [32]. The brackets signify that the order parameter is averaged over all C-C bonds in all acyl chains during the final 30 ns of the simulation. The order parameter along the C-C backbone was separately determined as a function of acyl bond number for each GMO concentration. An order parameter could not be defined for the PGPR molecules, given their polymeric arrangement. Results are taken from a single simulation run but averaged over the two independent interfaces in the simulation box.

## 3. Results and Discussion

The structure and organisation of mixed TS-water interfacial layers with either GMO or PGPR were studied over a surface coverage ($\Gamma$) range from 0.21-1.67 mg/m$^2$ for GMO (100-800 molecules per simulation) and 0.33-1.64 mg/m$^2$ for PGPR (40-200 PGPR molecules per simulation). This range was below the saturated surface coverage for adsorbed GMO molecules ($\sim$ 2.17 mg/m$^2$),

which we interpolated from Lutton et al. (1969) for monostearin monolayers at the TAG oil-water interface, which they believe corresponded to a solid or condensed liquid layer with area per molecule $\sim 25$ Å$^2$ [25].

Figure 2 depicts snapshot conformations along (first column) and normal to the interface (second and third columns) after 600 ns of the GMO systems, with and without TS, at surface coverages of 0.21 (a-c), 1.04 (d-f), and 1.67 mg/m$^2$ (g-i). It is apparent that, in the absence of TS, GMO beads (pink) cluster at the interface with their acyl chains (blue and grey) pointing into the void space. At lower GMO concentrations, TS GOH beads (yellow) can fill the empty interfacial space but additional GMO molecules will supplant TS at the interface. At the highest $\Gamma$, the GMO GOH groups nearly completely occupy the TS-water interface; this is to be expected given the lack of TS surface activity compared to the surfactant.

At the lowest $\Gamma$, the large GMO clusters that form in the absence of TS do not materialise in the TS-water systems (e.g., Figure 2b vs. c). This may be surprising considering phase separation of phospholipids in monolayers and bilayers has been observed using MD techniques [33]. Phase separation is observed in phospholipid membranes when the two components have different melting temperatures; in this case, differences in the degree of unsaturation will affect the components melting temperatures [34]. However, Voronoi analysis of our median area per molecule at these low concentrations is at or above the area per lipid for the liquid expanded phase (see Supplemental Information), whereas phase separation of phospholipids is more evident in a liquid condensed phase [33]. Phase separation is more apparent at higher GMO $\Gamma$ when the median area per molecule of the TS-water systems starts to approach that of the air-water systems. Any tendency towards phase separation in a GMO+TS mixed monolayer may be driven partly by the differing saturation degree of the acyl chains and partly by differing hydrophilicity of the two head groups.

Figure 3 shows a wireframe model of the TS-water interface at a GMO surface coverage of 1.04 mg/m$^2$ GMO, where the GMO molecules are pink, purple, and blue to denote the GOH, ester bead, and acyl chain, respectively.

The TS molecules are white. It is apparent that TS interacts with the GMO monolayer in two ways. Some TS molecules embed themselves into the GMO acyl chains with their three acyl chains oriented away from the interface. This conformation has been observed experimentally at the air-water interface for tripalmitin, tristearin and triarachidin [35, 36] and in simulations at the TS-water interface [18], and has been termed the trident conformation (Figure 3d oval). Other TS molecules have their GOH head bead located further from the surface, with some acyl chains that penetrate into the acyl chain layer of the GMO monolayer and others that point the opposite direction into the bulk TS phase.

The density of the GOH head group of the TS molecules interacting with the GMO layer is plotted normal to the interface for four GMO $\Gamma$ values in Figure 4. At $\Gamma \leq 1.25$ mg/m$^2$, the TS GOH beads have two peaks in the density profile, one at the water interface and a second $\sim 3$ nm from the surface. At $\Gamma = 1.67$ mg/m$^2$, the first GOH peak disappears and only the second peak further from the surface is seen. At lower $\Gamma$ values, the area occupied per molecule by the GMO is above that of the close packed monolayer. This allows the TS molecules to interdigitate into the GMO layer thus increasing the number of TS molecules in the adsorbed layer, leading to the peak at the water interface at $\Gamma \leq 1.25$ mg/m$^2$. The extra space available also allows some TS molecules to penetrate into the GMO layer and for their GOH head group to occupy space in the interfacial region. At the highest $\Gamma$ value, there is less space for TS, and the TS GOH head group is excluded from the interfacial region. A likely reason for this exclusion of the TS GOH bead from the interface is due to the polar nature of the GMO GOH and the non-polar nature of the TS GOH, given the absence of OH groups in the latter. In a dense GMO layer, the GOH beads will interact via electrostatic interactions between the partial charges that reflect the dipole-dipole interactions between the glycerol head groups of GMO, thus forming a condensed liquid or perhaps solid-like layer. As the TS GOH bead cannot hydrogen bond with the GMO GOH, any TS GOH bead in the adsorbed GMO layer would lead to an unfavourable disruption of the hydrogen-bonded

network.

The orientation of acyl chains in the adsorbed layer is expressed as the mean order parameter. Figure 5 shows the mean order parameter averaged over each individual C-C bond in the acyl chain of the GMO and averaged over all C-C bonds in all three acyl chains of the TS molecule. The TS molecules are separated into three populations: those whose GOH bead is at the TS-water interface ("TS in interface"), those whose acyl chains are interacting through interdigitation of the GMO monolayer ("TS other"), and all of the TS molecules in the simulation ("TS all"). In addition, results from a separate simulation of only TS and water were plotted to determine if TS molecules in contact with a water surface are ordered at the interface. The acyl chains of GMO and TS at the interface have positive order parameters at all values indicating they are more closely aligned to the perpendicular of the interface. As increases, so does the order parameter of the interdigitated TS, indicating that as the GMO concentration nears monolayer coverage, it is able to induce order in neighbouring TS molecules. This supports the templating effect previously observed experimentally during the crystallisation of TAGs in the presence of molecularly-similar MAGs [11, 37]. With or without GMO, the mean order parameter for all TS molecules is low but positive non-zero, which suggests the total ensemble of TS molecules is slightly ordered. This could occur because when calculating the order parameter, it contains some interfacial TS, which is more ordered than the total TS, and thus contributes to an increased order parameter. In the absence of GMO, the TS molecules at a water interface have increased acyl chain order compared to the total TS (bulk + interfacial), indicating that TS molecules in contact with the interface adopt different conformations than in the bulk phase. This conformation is the trident conformation mentioned above [35, 36]. Still, the GMO clearly aids in orienting the TS perpendicularly to the interface, as the order parameter of TS in the presence of GMO is consistently above that of the surfactant-free system.

Figure 5 exhibits a slight dip in interfacial TS order parameter at $0.6 < \Gamma < 1.5$ mg/m$^2$. As only a few TS molecules have their GOH bead at the inter-

face at the highest GMO concentration, it proved difficult to study. For the GMO at the air-water interface, a drop in the order parameter occurred at Γ around 1.46 mg/m$^2$ (Figure 5 inset). In this concentration range, the GMO in an air-water system undergoes a transition from incomplete surfactant coverage to a full monolayer in which all nearest neighbours are separated by lengths less than the interaction cutoff (1.2 nm). This leads to fewer beads with a planar orientation ($S_{CD}$ = -0.5) yet an increase in beads with isotropic orientation ($S_{CD}$ = 0). We find that while the average nearest-neighbour distance decreases with increasing Γ, the fraction of total nearest-neighbour distances that are short (< 0.7 nm) actually decreases. One would expect the opposite as Γ increases: more GMO at the interface should result in a larger population of shorter nearest-neighbour distances. As the largest gaps in the surfactant layer are filled, a few GMO molecules with planar orientation localised near the holes in the surfactant layer have been replaced by homogeneous isotropic order, leading to smaller highly ordered clusters (see Supplemental Information). Pohrille & Wilson (1995) have simulated GMO bilayers at the air-water interface and have observed that the membranes fluctuate over time; occasional membrane thinning and pore formation is observed [38].

As for the TS-water system, the packing transition is not as obvious, but the dip in order parameter corresponds to a point where the standard deviation of the nearest-neighbour distances for the TS GOH beads suddenly increases by 50% compared to the value at 1.25 mg/m$^2$, deviating greatly from the trend of decreasing standard deviation with increasing concentration. Comparatively, the standard deviation of the nearest-neighbour distances of just the GMO GOH beads is nearly identical to that of the TS GOH beads at 1.25 mg/m$^2$ but more than 1.5× greater for the TS GOH beads at 1.46 mg/m$^2$. However, the mean values for both GOH populations consistently decrease with increasing GMO concentration. We suggest this indicates that around 1.46 mg/m$^2$, the GMO molecules reach a concentration and separation length at which their preferential van der Waals interactions dominate at the expense of GMO-TS acyl chain interactions, giving TS molecules more space to orient their acyl

chains isotropically with respect to the interface normal.

The order parameter of the TS-water system for GMO molecules along the carbon backbone is shown in Figure 6. It is clear that the order decreases moving away from the TS-water interface. All concentrations show positive order parameters at the first carbon, while the double bond eradicates any residual order. Rather than showing a clear increase in order with greater surface coverage, the systems are virtually indistinguishable aside from the highest concentration at 1.67 mg/m$^2$.

The structure of the adsorbed layer for PGPR at a TS-water interface is shown in Figure 7 for PGPR  values of 0.33 (a-c), 0.98 (d-f) and 1.64 mg.m-2(g-i). The first column of Figure 7 views the system along the interface while the second and third columns are viewing normal to the interface. At the TS-water interface (columns 1-2), PGPR does not form an ordered monolayer in the same way that GMO does but adopts a layer of disordered, entangled chains that appear more like that formed by a polymer. It is apparent that the TS molecules (yellow) interact differently with this layer. The number of TS molecules sharing the interfacial region with the PGPR molecules is greater than for a GMO adsorbed layer. Some TS molecules do occupy space close to the water phase with their GOH head bead in contact with water, but what is absent is the two layers of TS molecules (one close to the interface, one interacting with the acyl chain of GMO) as seen in GMO simulations. It is also evident that the TS molecules that do interact with the PGPR layer are more disordered than those in a GMO layer or those at a TS-water interface.

The mean order parameter for TS interacting with the PGPR adsorbed layer is shown in Figure 8. The order parameter for interfacial TS acyl chains in PGPR systems is clearly lower than those in GMO systems (Figure 5) and is only marginally higher at a given PGPR $\Gamma$ than the entire TS population. No order parameter can be defined for the PGPR molecules since it lacks distinct acyl chains, so it cannot be concluded just from the order parameter alone that the lack of ordering of the TS acyl chains is due to a lack of order in the PGPR layer. However, it is clear that more PGPR located at the interface reduces

whatever ordering that exists in the TS molecules until the arrangement of TS acyl chains at the interface matches that of bulk TS molecules. As a result, there exists no ordered structure at the interface to serve as a template to promote interfacial crystallisation of bulk TS, supporting earlier experimental results.

## 4. Conclusions

We have simulated the oil-water and air-water interfaces in the presence of either GMO or PGPR. At similar $\Gamma$ values, they have opposite effects on the bulk TS phase; GMO tends to promote ordering normal to the interface while PGPR reduces any ordering that would otherwise exist at a bare interface. Mutual interfacial ordering of GMO and TS acyl chains leads to ordered structures (i.e., trident TAG conformation) forming adjacent to the interface. Any bulk phase ordering is more apparent at higher GMO concentrations. Our results bolster the experimental observations that surfactants with a complementary structure such as GMO induce TAG ordering and crystallisation at the oil-water interface while branched, polymeric surfactants such as PGPR displace TAGs thus limiting any tendency towards interfacial crystallisation.

## Acknowledgements

DR acknowledges financial support from the Natural Sciences and Engineering Research Council of Canada (NSERC).

## References

[1] D. J. McClements, Annu. Rev. Food Sci. Technol. 1 (2010) 241. doi:10.1146/annurev.food.080708.100722.

[2] B. J. D. Le Révérend, M. S. Taylor, I. T. Norton, Int. J. Cosmet. Sci. 33 (2011) 263. doi:10.1111/j.1468-2494.2010.00624.x.

[3] R. P. Borwankar, L. A. Frye, A. E. Blaurock, F. J. Sasevich, J. Food Eng. 16 (1992) 55. doi:10.1016/0260-8774(92)90020-7.

[4] D. Rousseau, L. Zilnik, R. Khan, S. Hodge, J. Am. Oil Chem. Soc 80 (2003) 957. doi:10.1007/s11746-003-0803-0.

[5] D. Johansson, B. Bergenståhl, E. Lundgren, J. Am. Oil Chem. Soc. 72 (1995) 921. doi:10.1007/BF02542070.

[6] N. Krog, K. Larsson, Fat Sci. Technol. 2 (1992) 55. doi:10.1002/lipi.19920940205.

[7] S. Ghosh, T. Tran, D. Rousseau, Langmuir 27 (2011) 6589. doi:10.1021/la200065y.

[8] I. Foubert, B. Vanhoutte, K. Dewettinck, Eur. J. Lipid Sci. Technol. 106 (2004) 531. doi:10.1002/ejlt.200400979.

[9] M. S. Aston, T. M. Herrington, T. F. Tadros, Colloid Polym. Sci. 273 (1995) 444. doi:10.1007/BF00656889.

[10] P. Wassell, A. Okamura, N. W. G. Young, G. Bonwick, C. Smith, K. Sato, S. Ueno, Langmuir 28 (2012) 5539. doi:10.1021/la204501t.

[11] S. Ghosh, D. Rousseau, Cryst. Growth Des. 12 (2012) 4944. doi:10.1021/cg300872m.

[12] P. Poulin, D. A. Weitz, Phys. Rev. E 57 (1998) 626. doi:10.1103/PhysRevE.57.626.

[13] J. M. Brake, N. L. Abbott, Langmuir 18 (2002) 6101. doi:10.1021/la011746t.

[14] N. A. Lockwood, J. J. de Pablo, N. L. Abbott, Langmuir 21 (2005) 6805. doi:10.1021/la050231p.

[15] J. M. Brake, A. D. Mezera, N. L. Abbott, Langmuir 19 (2003) 6436. doi:10.1021/la034132s.

[16] J. Chanda, S. Bandyopadhyay, J. Phys. Chem. B. 110 (2006) 23482. doi:10.1021/jp063205o.

[17] A. M. Tikonov, S. V. Pingali, M. L. Schlossman, J. Chem. Phys. 120 (2004) 11822. doi:10.1063/1.1752888.

[18] Z. E. Hughes, T. R. Walsh, RSC Adv. 5 (2015) 49933. doi:10.1039/c5ra09192f.

[19] S. Wang, R. G. Larson, Langmuir 31 (2015) 1262. doi:10.1021/la503700c.

[20] M. Ndao, F. Goujon, A. Ghoufi, P. Malfreyt, Theor. Chem. Acc. 136 (2017) 21. doi:10.1007/s00214-016-2038-y.

[21] P. Larsson, L. C. Alskär, C. A. S. Bergström, Mol. Pharmaceutics 14 (2017) 4145. doi:10.1021/acs.molpharmaceut.7b00397.

[22] B. Hess, C. Kutzner, D. van der Spoel, E. Lindahl, J. Chem. Theory Comput. 4 (2008) 435. doi:10.1021/ct700301q.

[23] S. J. Marrink, H. J. Risselada, S. Yefimov, D. P. Tieleman, A. H. de Vries, J. Phys. Chem. B 111 (2007) 7812. doi:10.1021/jp071097f.

[24] T. Vuorela, A. Catte, P. S. Niemelä, A. Hall, M. T. Hyvönen, S. J. Marrink, PLoS Comput. Biol. 6 (2010) e1000964. doi:10.1371/journal.pcbi.1000964.

[25] E. S. Lutton, C. E. Stauffer, J. B. Martin, A. J. Fehl, J. Colloid Interface Sci. 30 (1969) 283. doi:10.1016/0021-9797(69)90395-6.

[26] M. Parrinello, A. Rahman, J. Appl. Phys. 52 (1981) 7182. doi:10.1063/1.328693.

[27] S. Nose, M. L. Klein, Mol. Phys. 50 (1983) 1055. doi:10.1080/00268978300102851.

[28] G. Bussi, D. Donadio, M. Parrinello, Int. J. Pharm. (Amsterdam, Neth.) 126 (2007) 014101. doi:10.1063/1.2408420.

[29] A. Hall, J. Repakova, I. Vattulainen, J. Phys. Chem. B. 112 (2008) 13772. doi:10.1021/jp803950w.

[30] A. Pizzirusso, A. Brasiello, A. D. Nicola, A. G. Marangoni, G. Milano, J. Phys. D: Appl. Phys. 48 (2015) 494004. doi:10.1088/0022-3727/48/49/494004.

[31] W. Maier, A. Saupe, Z. Naturforsch., A: Astrophys., Phys. Phys. Chem. 13 (1958) 564.

[32] E. Egberts, H. J. C. Berendsen, J. Chem. Phys. 89 (1988) 3718. doi:10.1063/1.454893.

[33] S. Baoukina, E. Mendez-Villuendas, D. P. Tieleman, J. Am. Chem. Soc. 134 (2012) 17543. doi:10.1021/ja304792p.

[34] D. Marsh, Biochim. Biophys. Acta, Biomembr. 1798 (2010) 40. doi:10.1016/j.bbamem.2009.10.010.

[35] T. Bursh, K. Larsson, M. Lundquist, Chem. Phys. Lipids 2 (1968) 102. doi:10.1016/0009-3084(68)90036-4.

[36] A. N. Zdravkova, J. P. J. M. van der Eerden, Cryst. Growth Des. 7 (2007) 2778. doi:10.1021/cg060701t.

[37] S. Verstringe, K. Dewettinck, S. Ueno, K. Sato, Cryst. Growth Des. 14 (2014) 5219. doi:10.1021/cg5010209.

[38] A. Pohorille, M. A. Wilson, Origins Life Evol. Biosphere 25 (1995) 21. doi:10.1007/BF01581571.

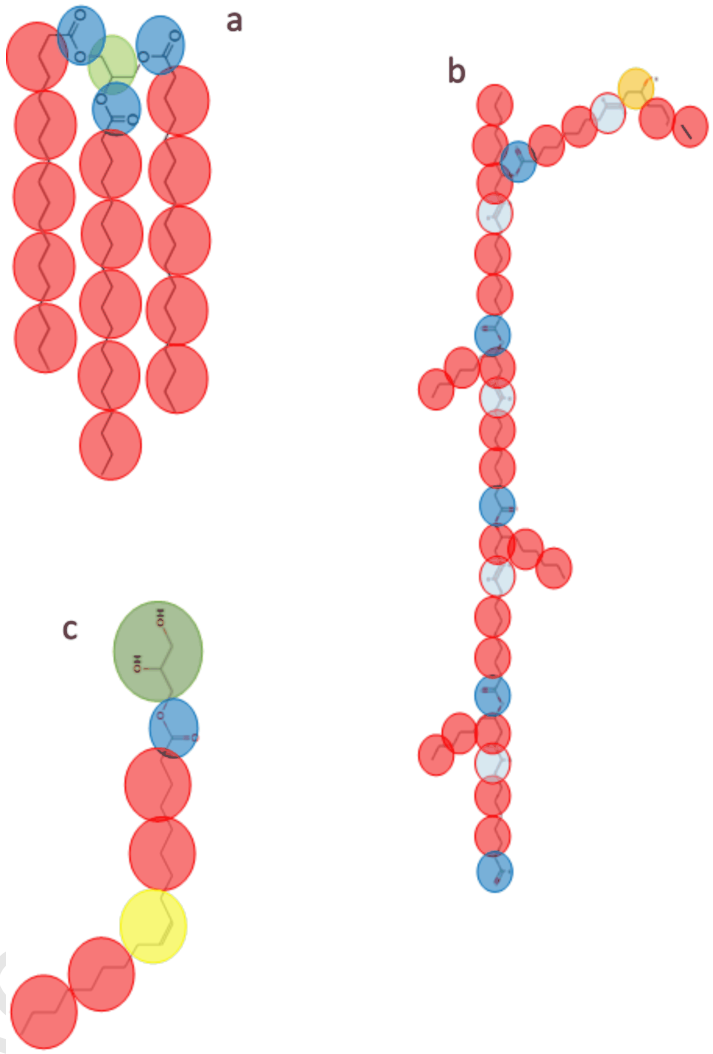


Figure 1: Coarse-grained representation of (a) tristearin (TS), (b) polyglycerol polyricinoleate (PGPR) and (c) glycerol monooleate (GMO) using the Martini coarse-grained force field representation. Red corresponds to CG bead type C1, yellow to C3, blue to Na and green to P1 [23].

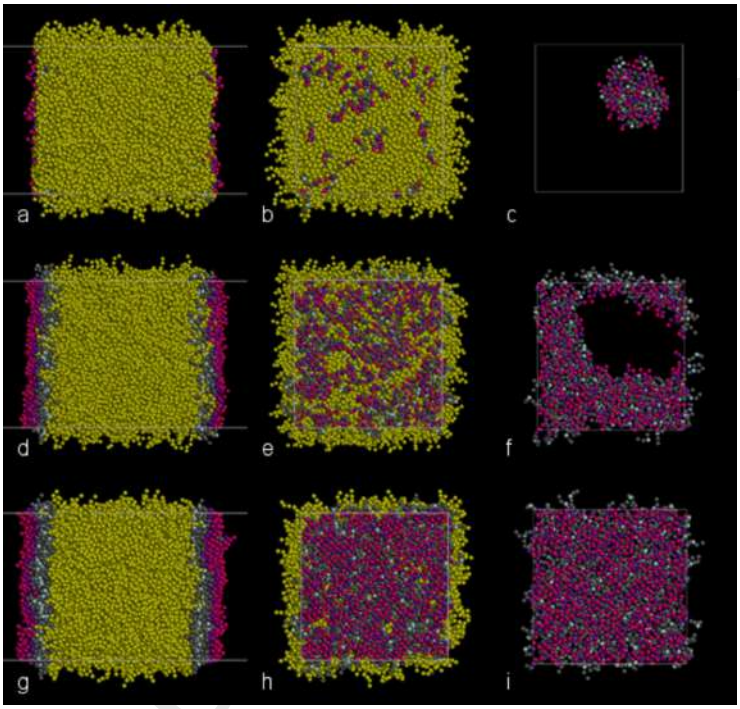


Figure 2: Snapshot conformations of GMO at TS-water (a,b,d,e,g,h) and air-water (c,f,i) interface after 600 ns of simulation time. Three GMO Γ values are represented: (a–c) 0.21 mg/m$^2$; (d–f) 1.04 mg/m$^2$; and (g–i) 1.67 mg/m$^2$. Images are looking along the interface in the first column and perpendicular to one interface in the other two columns. TS molecules are coloured yellow. GMO molecules have the GOH bead coloured pink, the ester bead purple, and the acyl chain beads grey and light blue. The light blue acyl chain bead signifies the position of the *cis* double bond. Water beads have been removed for clarity.

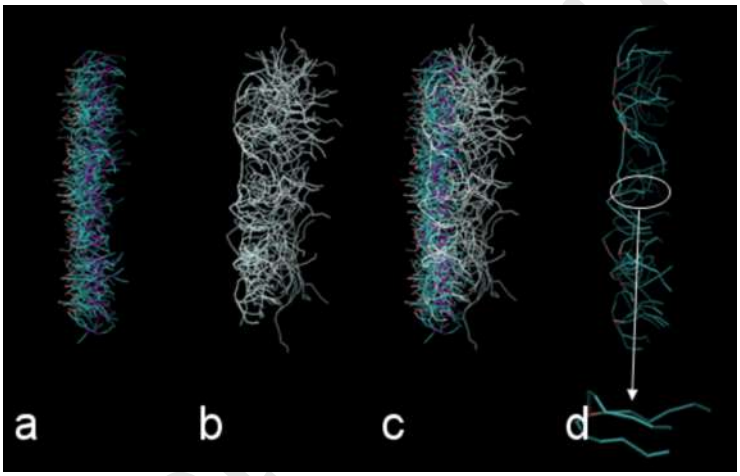


Figure 3: Structure of the mixed interfacial layer at a TS-water interface at GMO $\Gamma$=1.04 mg/m$^2$. The GMO (a), TS (b), and the overlay of the two (c) are shown as a wireframe representation. In (d) only the TS molecules with a GOH bead close to the interfacial region are shown, with one TS molecule highlighted to show the trident conformation.

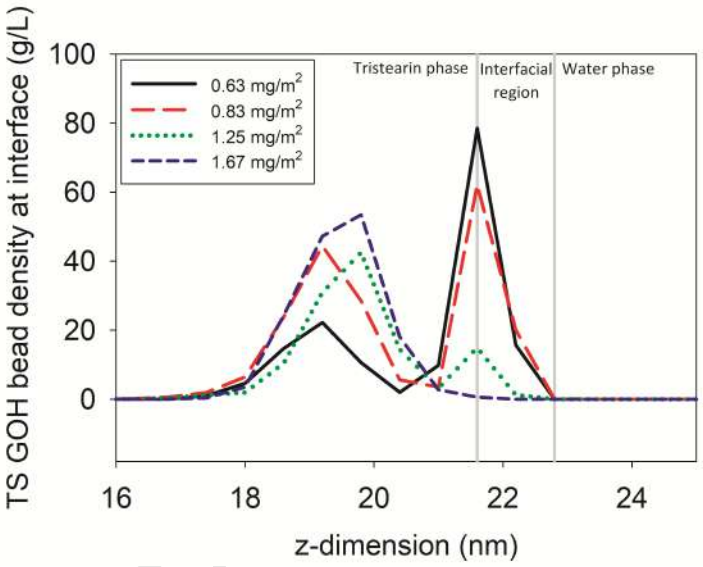


Figure 4: TS GOH bead density along the TS-water interface normal for 0.63, 0.83, 1.25, and 1.67 mg/m$^2$ GMO surface coverages. Only TS interacting with the GMO at the interface is plotted ("TS in interface" and "TS other" in Figure 5). Increasing GMO concentration excludes TS at the interface, while simultaneously greater acyl chain interaction between GMO and TS leads to a second TS GOH bead peak beyond the interface.

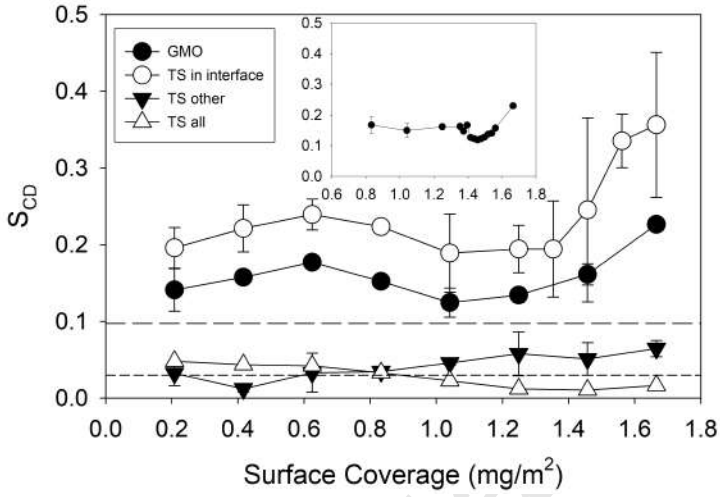


Figure 5: Average order parameter of GMO and TS acyl chains as a function of GMO surface coverage. • GMO, ○ TS with their GOH beads at the interface, ▼ TS molecules interacting with interfacially-located molecules, △ all TS in the system, —— TS at the interface in an surfactant-free system, and – – – all TS in a surfactant-free system. Inset: GMO order parameter at an air-water interface.

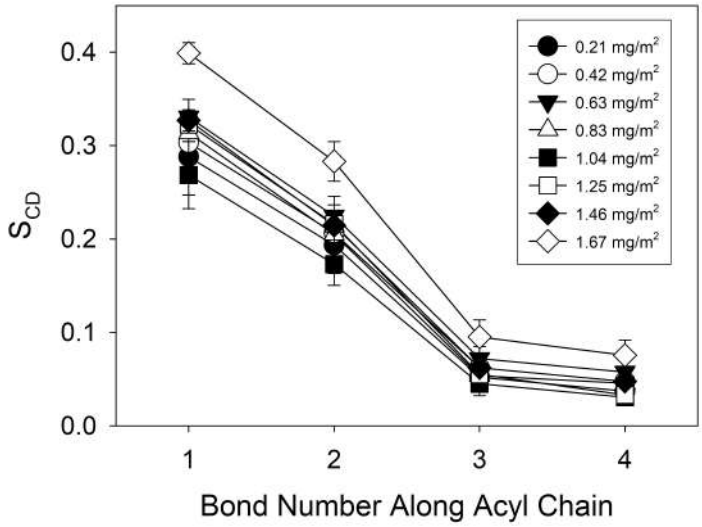


Figure 6: Average second rank order parameter ($S_{CD}$) calculated along the acyl chain of the GMO molecules in a TS-water system as a function of the GMO surface coverage.

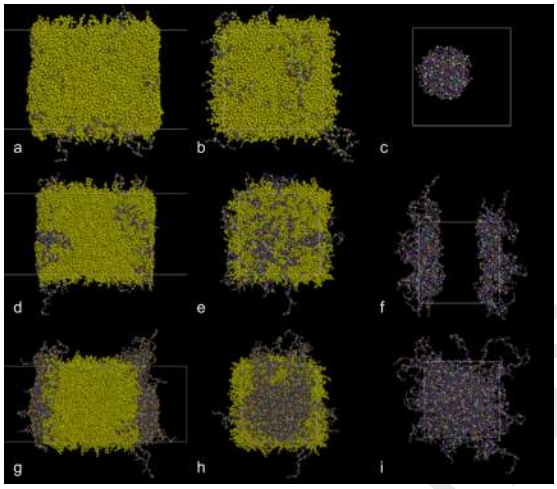


Figure 7: Snapshot conformation of PGPR at TS-water (a,b,d,e,g,h) and air-water (c,f,i) after 600 ns of simulation time. Three PGPR Γ values are represented: (a–c) 0.33 mg/m$^2$; (d–f) 0.98 mg/m$^2$; and (g–i) 1.64 mg/m$^2$. Images are looking along the interface in the first column and perpendicular to one interface in the other two columns. TS molecules are coloured yellow. All other beads are part of the PGPR molecules. Water beads have been removed for clarity.

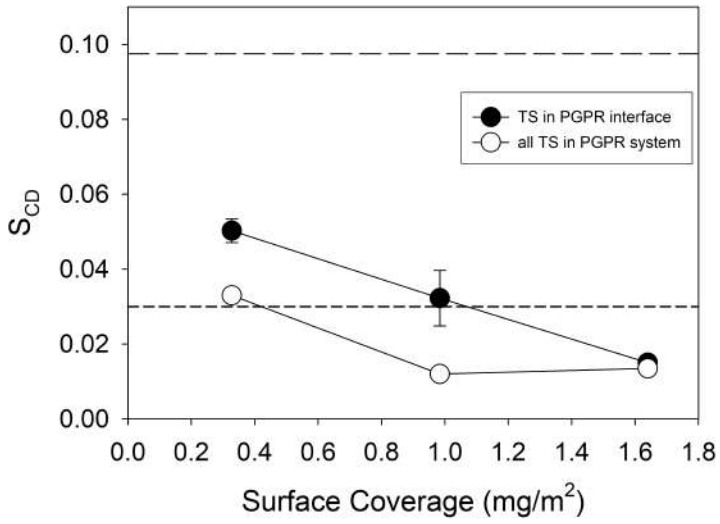


Figure 8: Average order parameter of TS acyl chains as a function of PGPR surface coverage. • TS interacting with interfacially-located molecules, ◦ all TS in the system, —— TS at the interface in an surfactant-free system, and – – – all TS in a surfactant-free system.

**Graphical Abstract**